Dependence of Shaft Stiffness on the Crack Location

H. M. Mobarak, Helen Wu, Chunhui Yang

Abstract—In this study, an analytical model is developed to study crack breathing behavior under the effect of crack location and unbalance force. Crack breathing behavior is determined using effectual bending angle by studying the transient change in closed area of the crack. The status of the crack of a balanced shaft is symmetrical about shaft rotational angle and the duration of each crack status remains unchanged. The global stiffness of the balanced shaft is independent of crack location. Different crack breathing behavior for the unbalanced shaft has been observed. The influence of crack location on the unbalanced shaft stiffness can be divided into three regions. When the crack is located between 0.3L and 0.8335L, where L is the total length of the shaft, the unbalanced shaft is less stiff and when located outside this region it is stiffer than the balanced shaft. It was also found that unbalanced shaft stiffness has a maximum value with a crack at 0.1946L, a minimum value at 0.8053L and same value as balanced shaft at 0.3L and 0.8335L.

Keywords—Cracked shaft, crack location, shaft stiffness, unbalanced force.

I. INTRODUCTION

BREATHING of the fatigue cracks are considered to be one of the main rotor faults in rotating machinery. It has a great deal of attention in literature as one of the main causes of dangerous damages in rotor systems [1]. A wide variety of analytical and practical methods have been used or developed for the detection of transverse rotor cracks [2]-[4]. Classic papers [5], [6] on cracked shaft literature used gaping crack models where the crack is considered to always be fully open. However, such a model does not represent the actual breathing of a fatigue crack. Improvements are seen through a switching crack model in a number of classic papers including [7], [8]. In switching crack model, the crack is considered either fully open or fully closed. Further, switching crack models are associated with chaotic and quasiperiodic vibrations that are not seen in experimental testing. Recently, a number of papers [9], [10] have used more realistic trigonometric functions to describe the crack breathing mechanism of a rotating shaft.

As mentioned above, numerous studies on cracked rotors are formed on the basis of a crack breathing mechanism under static loading, which disallows accurate modelling of crack breathing behavior under unbalance force. Moreover, almost all existing models are not applicable near the shaft critical speed because equations of motion developed under the assumption of rotor static load dominance are no longer suitable for analysis near the critical speed. As such, a few studies have examined some facets of non-linear crack breathing. Bachschmid et al. [11] study the non-linear breathing mechanism by significantly reducing the damping of the cracked rotor system as to amplify the influence of the breathing behavior of the crack. Cheng et al. [10] found that unbalance can restore the stability of a rotor. Rubio et al. [12] used commercial FEM software used to model the effects of mass unbalance on the breathing behavior of a cracked Jeffcott rotor with a crack.

An accurate analytical model is still absent which considers the coupling influence of both crack location and unbalance force on the crack breathing mechanism. This paper aims to develop an unbalanced shaft model to study the effect of crack location on the breathing behavior of the fatigue crack under unbalanced force. Firstly, the model describes the relative angle between the crack and shaft bending directions and then is used to find the breathing behavior of the crack at different crack locations by using the percentage of opening of a crack and examining the duration of each crack state (fully open, fully closed and partially open/closed). Results are also compared with those obtained using balanced model, which do not include the effect of unbalanced force.

II. CRACK BREATHING UNDER DYNAMIC LOADING

Regardless of the type of loading (static or dynamic), the breathing of a fatigue crack are governed by the effectual bending angle, φ, the proximity of the direction of the bending on the system relative to the crack direction. The model seen in Fig. 1 was developed to describe effectual bending angle of a system subject to cracking and mass unbalance for different crack locations. This model represents a two-disk rotor supported rigidly by two bearings. The model consists of a straight front oriented crack on a plane normal to the axis of the shaft as shown in Fig. 2, h is the crack depth in the radial direction and R is the shaft radius. The shaft total length, L, is equal to 724 mm, whereas the radius, R, is 6.35 mm. The material of shaft is steel with the following mechanical properties: density, ρ=7800 kg/m^3, Poisson ratio, v=0.3 and Young's Modulus, E=210 GPa.

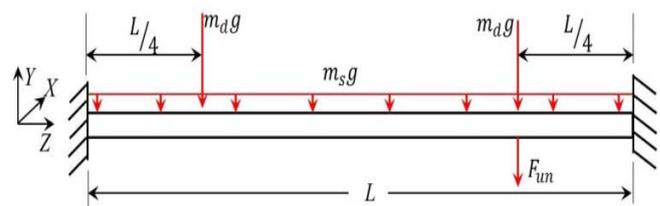Fig. 1 A rigidly supported two-disk rotor

H.M. Mobarak is with the Western Sydney University, Penrith NSW 2747, Australia (corresponding author, e-mail: mobarak.hossain@westernsydney.edu.au).

Helen Wu and Chunhui Yang are with the Western Sydney University, Penrith NSW 2747, Australia (e-mail: helen.wu@westernsydney.edu.au, r.yang@westernsydney.edu.au).

World Academy of Science, Engineering and Technology
International Journal of Mechanical and Mechatronics Engineering
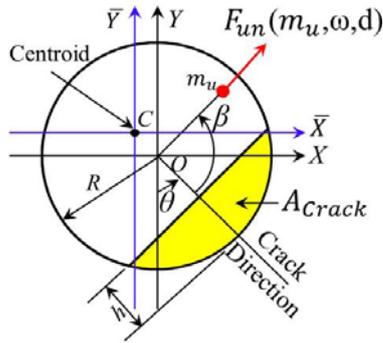Vol:11, No:2, 2017

Fig. 2 Relative position of the unbalanced force with respect to the crack

The static load due to the shaft weight $m_s g$ is uniformly distributed, where m_s is the mass of the shaft. The weight of two disks $2m_d g$ is static point load and m_d is the mass of each disk. The unbalance force, $F_{un} = m_u \omega^2 d$ is considered as the dynamic load due to the unbalance mass, m_u, located on the right disk as an additional mass at a radial distance d from the center of the shaft where ω is shaft rotation speed (see Fig. 2). The direction of the static forces due to disks and shaft always acts downward in the negative Y-axis. Therefore, the gravitational moments M_{mg1} and M_{mg2} due to $m_s g$ and $2m_d g$ respectively act perpendicular to the load direction along the negative X-axis. The rotational load F_{un} acts in the radial direction with a fixed angular position β relative to the crack direction. Therefore the direction of the rotational unbalance load F_{un} is $(\theta+\beta)$, where θ is the shaft rotation angle at time t and β is angular position of the unbalance force relative to the crack direction. The direction of the unbalance moment M_{un} due to F_{un} is perpendicular to the F_{un} (see Fig. 3) and rotates anticlockwise by ω. The gravitational moment M_{mg1} and M_{mg2} and unbalance moment M_{un} at crack location l_0 are described as:

$$M_{mg1} = \frac{m_s g}{12L} (6Ll_0 - L^2 - 6l_0^2) \text{ when } 0 \leq l_0 \leq L \quad (1)$$

$$\left. \begin{aligned} M_{mg2} &= m_d g l_0 - \frac{3m_d g L}{16} & \text{when } 0 \leq l_0 \leq \frac{L}{4} \\ M_{mg2} &= \frac{m_d g L}{16} & \text{when } \frac{L}{4} < l_0 < \frac{3L}{4} \\ M_{mg2} &= m_d g(L - l_0) - \frac{3m_d g L}{16} & \text{when } \frac{3L}{4} \leq l_0 \leq L \end{aligned} \right\} \quad (2)$$

$$\left. \begin{aligned} M_{un} &= \frac{5F_{un}l_0}{32} - \frac{3F_{un}L}{64} & \text{when } 0 \leq l_0 \leq \frac{3L}{4} \\ M_{un} &= \frac{27F_{un}}{32}(L - l_0) - \frac{9F_{un}L}{64} & \text{when } \frac{3L}{4} \leq l_0 \leq \frac{L}{4} \end{aligned} \right\} \quad (3)$$

According to the principle of superposition theory, the total moment at crack location l_0:

In X-axis: $\sum M_x = M_{mg1} + M_{mg2} + M_{un} \cos(\theta + \beta)$ (4)

In Y-axis:

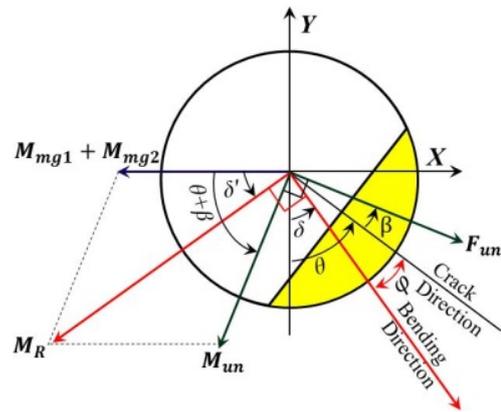$$\sum M_y = M_{un} \sin(\theta + \beta) \quad (5)$$

Fig. 3 A schematic representation of effectual bending angle

As shown in Fig. 3, bending direction of the shaft is perpendicular to the resultant moment direction. It should be pointed out that unbalance load F_{un} is not always located at the crack plane. Fig. 3 only represents a projection of F_{un} on the crack plane. The angle δ' of the resultant moment with X-axis is the same as δ of the bending direction with negative Y-axis. The effectual bending angle, φ described in (7) solely determines the breathing of the crack at any crack location. Modifications were made to ensure δ and φ are within the co-domain of full rotation of shaft values between 0 to 2π.

$$\delta = \tan^{-1}\left(\frac{\sum M_y}{\sum M_x}\right) \quad (6)$$

$$\varphi = \theta - \delta \quad (7)$$

The crack starts to close at a certain shaft rotation angle, θ, when the effectual bending angle $\varphi=\varphi_1$ where the upper end of the crack edge reaches the compression stress field as shown in Fig. 4 (a). The crack becomes fully closed at a certain shaft rotation angle when effectual bending angle $\varphi=\varphi_2$ where the crack is fully reached in the compression stress field as shown in Fig. 4 (b). φ_1 and φ_2 are given in (8) and (9) respectively, where μ is non-dimensional crack depth ratio h/R and e is the location of the centroid and A_1 is uncracked area as given in (10) and (11). Equations (8) and (9) were derived previously as shaft rotational angle to describe the crack breathing in the balanced shaft [13].

$$\varphi_1 = \tan^{-1}\left(\frac{e + R(1-\mu)}{R\sqrt{\mu(2-\mu)}}\right) \quad (8)$$

$$\varphi_2 = \frac{\pi}{2} + \cos^{-1}(1 - \mu) \quad (9)$$

$$e = \frac{2R^3}{3A_1} \sqrt[3]{\mu(2 - \mu)} \quad (10)$$

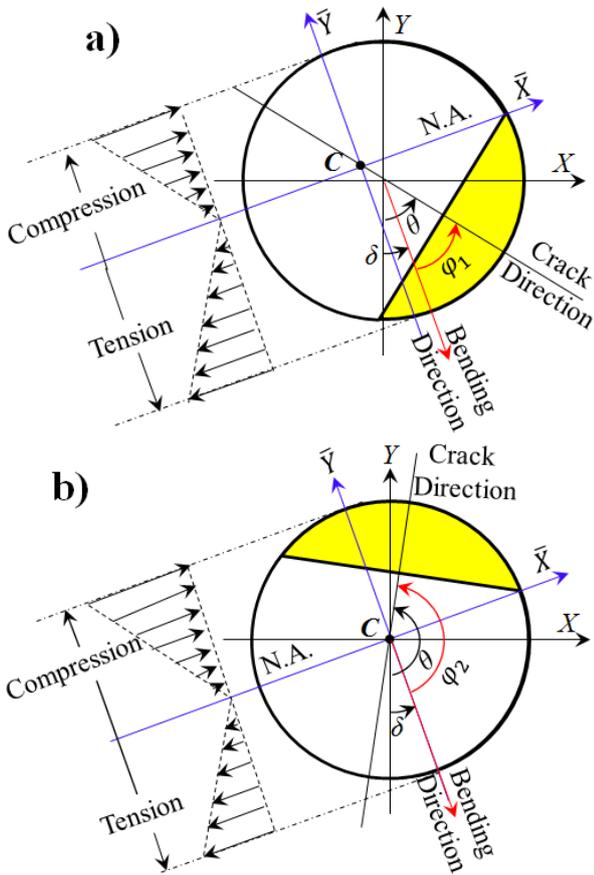$$A_1 = R^2\left[\pi - \cos^{-1}(1 - \mu) - (1 - \mu)\sqrt{\mu(2 - \mu)}\right] \quad (11)$$

World Academy of Science, Engineering and Technology
International Journal of Mechanical and Mechatronics Engineering
Vol:11, No:2, 2017

Fig. 4 Crucial angles for unbalanced shaft: (a) φ_1 crack begins to close and (b) φ_2 crack become fully closed
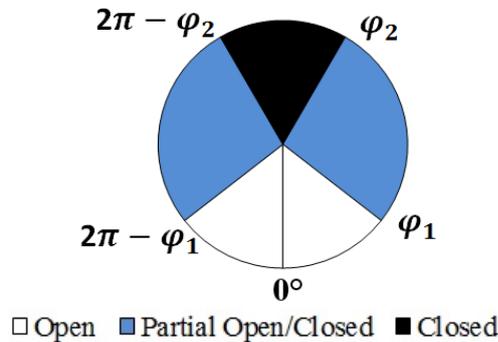

Fig. 5 Statuses of the crack breathing in the range of effectual bending angle from 0 degree to 2π

The statuses of the crack at different crack locations during shaft rotation are identified using the values of effectual bending angle relative to the regions formed by φ_1 and φ_2. Fig. 5 shows the full statuses of the crack breathing in the range of bending angle from 0 degree to 2π. The percentages of opening of cracks, Λ, (as described in (12)) are determined by studying the transient change in closed area of the crack. A_{crack} is the area of the crack segment at time zero as shown in Fig. 1 and $A_{closed}(t)$ is the closed portion of the crack segment when $\varphi_1 \leq \varphi \leq \varphi_2$ or $(2\pi-\varphi_2) \leq \varphi \leq (2\pi-\varphi_1)$ (see Fig. 6). A_{crack} can be calculated according to (13) and $A_{closed}(t)$ is determined using

the iterative procedure seen in [13]. For a fully open crack or fully closed crack the percentage of opening of a crack, Λ, is equal to 100 and 0, respectively.

$$\Lambda\ (\%) = \frac{A_{crack} - A_{closed}(t)}{A_{crack}} \times 100 \qquad (12)$$

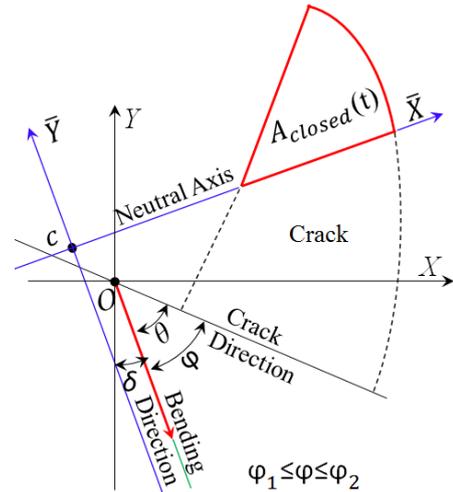$$A_{crack} = R^2 \cos^{-1}(1-\mu) - R^2(1-\mu)\sqrt{\mu(2-\mu)} \qquad (13)$$

Fig. 6 Schematic diagram of the closed portion of a breathing crack

III. RESULTS AND DISCUSSIONS

The breathing behavior of a crack in a shaft is related directly to the stiffness of the shaft. When a crack is fully closed the shaft will have a maximum stiffness and so it will be virtually identical to an intact shaft. Similarly, when a crack is fully opened the corresponding shaft stiffness will be at a minimum. For partially open/closed crack status the shaft stiffness is between the maximum and minimum values. In order to know the influences of crack location, the analysis has considered different crack location factors, λ, (the ratio of the crack position and shaft total length, L) with different force ratios, η (the ratio of the static force and the dynamic force). A series of analyses has been done using MATLAB. In this study the shaft rotation is anticlockwise and the initial crack direction aligns with the negative Y-axis. A crack with a depth ratio of $\mu=0.5$ and angular position of unbalance force relative to the crack direction, $\beta=0°$ is chosen to perform the analysis. Throughout the paper a focus is placed on the influences of the crack location on the status of the crack.

Fig. 7 describes the variation of percentage of opening of a crack along the shaft length. It is clear that crack opening and closing strongly depend on the crack location. For a balanced shaft crack opening percentage has a jump at crack locations 0.1946L and 0.8053L, respectively. This is caused by the change of gravitational moment direction which leads to a change of the shaft bending direction. It is seen that crack opening percentage in the balanced shaft in each of three regions divided at 0.1946L and 0.8053L remain unchanged. However, the variation sequence of the status of the crack in the middle region during a shaft revolution is opposite to that

World Academy of Science, Engineering and Technology
International Journal of Mechanical and Mechatronics Engineering
Vol:11, No:2, 2017

when the crack is situated at side regions, as shown in Fig. 8. When the crack is located at *0.5L* (middle region), the crack follows a sequential change from fully open, partially open/ closed, fully closed, partially open/closed and then fully open again. When the crack is located at *0.125L* (side region), the crack follows a sequential change beginning with a fully closed status. Further, the status of the crack in a balanced shaft during a shaft rotation is symmetrical (first half same as second half of the shaft rotation). Shaft stiffness during a full shaft rotation would be the same regardless of the crack location [14].
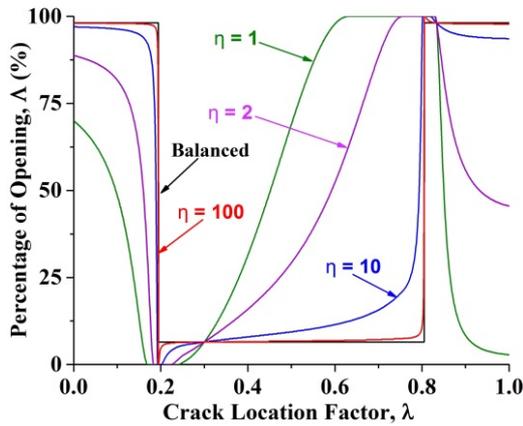

Fig. 7 Percentage of opening of a crack as a function of crack location for different force ratios where shaft rotation angle *135°*
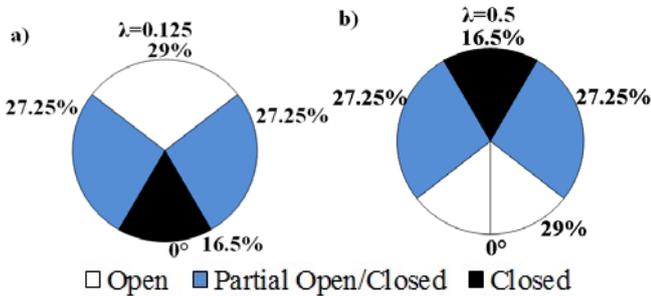

Fig. 8 Statuses of a crack in the balanced shaft during a shaft rotation at crack locations (a) $\lambda = 0.125$ and (b) $\lambda=0.5$

For an unbalanced shaft as shown in Fig. 7, the variation of percentage of opening of a crack along the shaft length is remarkably different from the balanced shaft. At crack locations *0.1946L* or *0.8053L*, it is independent of the force ratios, η. At former location, the crack is fully closed just like an uncracked shaft and the crack will never open during shaft rotation (see Fig. 9). The shaft will have a maximum stiffness and becomes virtually identical to an intact shaft. At the latter location *0.8054L*, the crack is fully open just like a shaft with a notch and will never close during shaft rotation. The shaft will have a minimum stiffness. The variation of opening percentage along shaft length can be clearly divided into three regions at *0.3L* and *0.8335L*. In the middle region, it is obvious that the percentage of opening of the crack for the unbalanced shaft is larger than that for the balanced

counterpart, which indicates that the balanced shaft is stiffer than the unbalanced shaft. And when the crack is located in two side regions, the percentage of opening is clearly lower than the balanced shaft, so unbalanced shaft is stiffer than the balanced shaft. This conclusion is drawn at a specific shaft rotational angle of *135* degree. However, this conclusion holds true during a full shaft rotation, as will be discussed later.
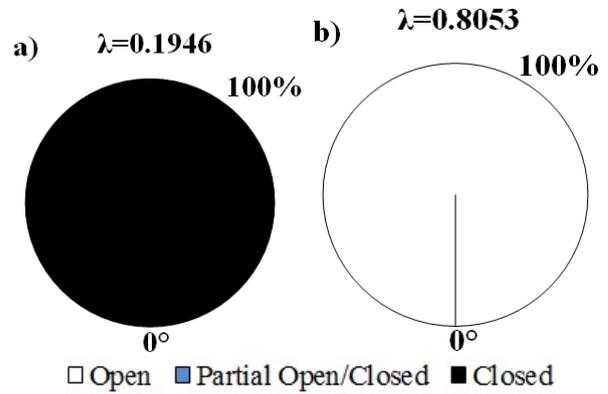

Fig. 9 Statuses of a crack in the unbalanced shaft during a shaft rotation at crack locations (a) $\lambda = 0.1946$ and (b) $\lambda = 0.8054$

The other interesting pair of crack locations are at *0.3L* and *0.8335L*, where the percentages of opening of a crack for all force ratios intersect at the same value for the balanced shaft (see Fig. 7). As a result, the cracks will breathe as they would in a balanced shaft. Therefore, unbalanced shaft stiffness would be the same as the balanced shaft. If the crack is located around these two positions then the effect of unbalance force on the crack breathing behavior can be ignored. However, the variation sequence of the crack status with shaft rotation is opposite to each other at these two crack locations, as shown in Fig. 10.
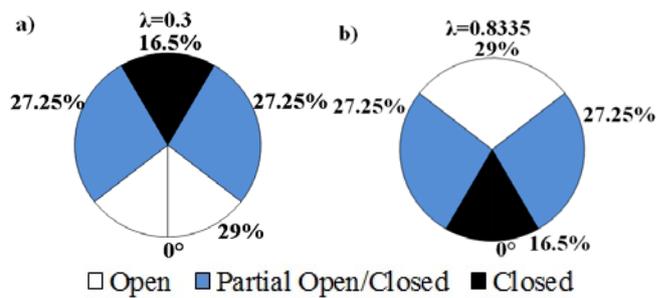

Fig. 10 Statuses of a crack in the unbalanced shaft during a shaft rotation at crack locations (a) $\lambda = 0.3$ and (b) $\lambda = 0.8335$

Figs. 11 and 12 show the statuses of a crack with different force ratios during a full shaft rotation at crack locations *0.5L* and *0.125L*, respectively. As the unbalance force decreases (i. e. force ratio increases) the angular range of either closed crack status or opened crack status will progressively approach those for the balanced shaft (comparing with Fig. 8), which demonstrates that the unbalanced model will be finally in agreement with a balanced model when force ratio is large

World Academy of Science, Engineering and Technology
International Journal of Mechanical and Mechatronics Engineering
Vol:11, No:2, 2017

enough. This conclusion can also be drawn from percentage of opening as seen in Fig. 7. Comparing Figs. 11 and 12, it was found that the angular range of the opened crack status for a given η during a complete shaft rotation at crack location $0.5L$ is much wider than that at $0.125L$, which is consistent with previous conclusion that the unbalanced shaft with crack at middle region is more flexible than the balanced shaft.
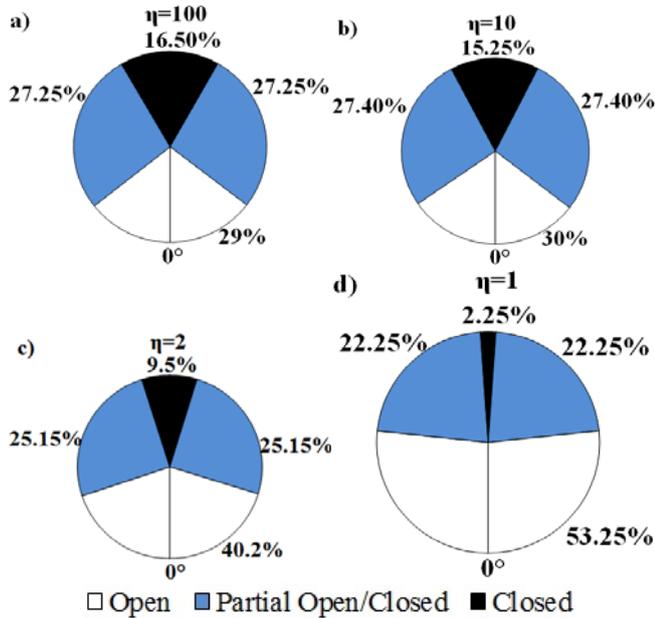

Fig. 11 Statuses of a crack during a shaft rotation at crack location λ = 0.5 for different force ratios (a) η = 100, (b) η = 10, (c) η = 2 and (d) η = 1
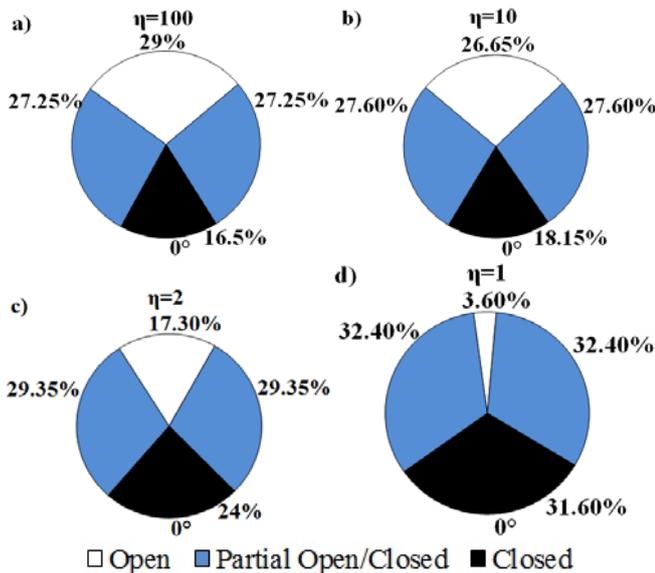

Fig. 12 Statuses of a crack during a shaft rotation at crack location λ = 0.125 for different force ratios (a) η = 100, (b) η = 10, (c) η = 2 and (d) η = 1

IV. CONCLUSIONS

In this study, a new analytical model is developed to study the effects of crack location on the shaft stiffness. The effectual bending angle was introduced to describe the breathing behavior of a crack (open, partial open/closed, closed and percentages of opening of a crack) at different crack location and it is further used to determine the transient change in closed area of the crack to examine the percentages of opening.

It was found that the transition sequence of the crack status in a balanced shaft is symmetrical about shaft rotation and is opposite to each other when the crack is in the middle region or side regions. The angular range of each crack status and the global stiffness of the balanced shaft remain unchanged regardless of crack location.

Notably different crack breathing behaviors have been identified for the unbalanced shaft. At crack location $0.1946L$ a crack is fully closed and the crack will never open. On the other hand at crack location $0.8053L$ the crack is fully open and the crack will never close. Shaft stiffness would be maximum at the former crack location and minimum at latter location. At either crack location $0.3L$ or $0.8335L$, an unbalanced shaft is behaves completely like a balanced shaft, the stiffness would be the same as the balanced shaft. For other crack locations unbalanced shaft stiffness would be between maximum and minimum values. Unbalanced shaft stiffness variation with crack location can be divided into three regions at crack locations $0.3L$ and $0.8335L$. When the crack is located in the middle region the unbalanced shaft is more flexible than the balanced shaft and stiffer when the crack is in the two remaining regions. As the unbalance force decreases, the breathing behavior of a crack in the unbalanced shaft will gradually approach that in the balanced shaft.

The developed new model can be further used to obtain the time-varying stiffness matrix of the cracked shaft element consisting of area moments of inertia and then to investigate the vibration behavior of the cracked rotor by solving the equation of motions.

REFERENCES

[1] S.K. Georgantzinos and N.K. Anifantis, An insight into the breathing mechanism of a crack in a rotating shaft. Journal of Sound and Vibration, 2008. 318: p. 279–295.
[2] Ming, L., et al., Multi-fault diagnosis of rotor system based on differential-based empirical mode decomposition. Journal of Vibration and Control, 2013: p. 1077546313502505.
[3] Kulesza, Z., Dynamic behavior of cracked rotor subjected to multisine excitation. Journal of Sound and Vibration, 2014. 333(5): p. 1369-1378.
[4] Yan, G., et al., A novel approach to detecting breathing-fatigue cracks based on dynamic characteristics. Journal of Sound and Vibration, 2013. 332(2): p. 407-422.
[5] Dimarogonas, A. and C. Papadopoulos, Vibration of cracked shafts in bending. Journal of Sound and Vibration, 1983. 91(4): p. 583-593.
[6] Papadopoulos, C. and A. Dimarogonas, Coupled longitudinal and bending vibrations of a rotating shaft with an open crack. Journal of sound and vibration, 1987. 117(1): p. 81-93.

[7] Sekhar, A.S., Crack detection through wavelet transform for a run-up rotor. Journal of Sound and Vibration, 2003. 259(2): p. 461-472.

[8] Sinou, J.-J., Effects of a crack on the stability of a non-linear rotor system. International Journal of Non-Linear Mechanics, 2007. 42(7): p. 959-972.

[9] Sinou, J.-J., Detection of cracks in rotor based on the 2× and 3× super-harmonic frequency components and the crack–unbalance interactions. Communications in Nonlinear Science and Numerical Simulation, 2008. 13(9): p. 2024-2040.

[10] Cheng, L., et al., The influence of crack breathing and imbalance orientation angle on the characteristics of the critical speed of a cracked rotor. Journal of Sound and Vibration, 2011. 330(9): p. 2031-2048.

[11] Bachschmid, N., P. Pennacchi, and E. Tanzi, Cracked rotors: a survey on static and dynamic behaviour including modelling and diagnosis. 2010: Springer Science & Business Media.

[12] Rubio, L., et al., Quasi-static numerical study of the breathing mechanism of an elliptical crack in an unbalanced rotating shaft. Latin American Journal of Solids and Structures, 2014. 11: p. 2333-2350.

[13] Al-Shudeifat, M.A. and E.A. Butcher, New breathing functions for the transverse breathing crack of the cracked rotor system: Approach for critical and subcritical harmonic analysis. Journal of Sound and Vibration, 2011. 330(3): p. 526-544.

[14] Mobarak, H.M. and H. WU, Crack breathing as a function of crack location under the effect of unbalance force. 24th Australasian Conference on the Mechanics of Structures and Materials (ACMSM24), Perth, Australia, 2016.